Green Chemistry

PAPER

Gold nanoparticles stabilized on nanocrystalline magnesium oxide as an active catalyst for reduction of nitroarenes in aqueous medium at room temperature†

Keya Layek,[a] **M. Lakshmi Kantam,**[*a] **Masayuki Shirai,**[b] **Daisuke Nishio-Hamane,**[c] **Takehiko Sasaki**[d] **and H. Maheswaran**[a]

Gold nanoparticles deposited on nanocrystalline magnesium oxide is a very efficient catalyst for the reduction of nitroarenes in aqueous medium at room temperature. Sodium borohydride is used as the source of hydrogen for the reduction of nitro groups. This catalytic system selectively reduces the nitro group even in the presence of other sensitive functional groups under very mild conditions in good to excellent yields without the requirement of any promoters. The reaction kinetics of reduction of 4-nitrophenol to 4-aminophenol has been studied by UV-visible spectrophotometry, and its apparent rate constant has been determined and compared with those of other supported gold catalysts. The spent heterogeneous catalyst is recovered by simple centrifugation, and reused for multiple cycles.

Introduction

Until the 1960s, gold was considered to be catalytically inert for hydrogenation reactions because it could not adsorb most molecules from the gas phase.[1] But a major breakthrough in gold catalyzed hydrogenation emerged when it was realized that gold, when dispersed in the form of nanoparticles on suitable oxide supports, could catalyze selective hydrogenation even in complex organic molecules containing multiple functional groups.[2]

Among the hydrogenation reactions catalyzed by gold nanoparticles, catalytic hydrogenation of aromatic nitro compounds to its corresponding amines is a very important reaction because functionalized anilines are industrially very important intermediates for pharmaceuticals, polymers, herbicides and other fine chemicals.[3] So, there is a strong need to develop suitable chemoselective catalysts for the reduction of nitro groups in the presence of sensitive functional groups involving green chemistry protocols.

Corma *et al.* has successfully demonstrated that gold nanoparticles supported on TiO_2 or Fe_2O_3 catalyze the chemoselective hydrogenation of functionalized nitroarenes with H_2 without the requirement of any additives or surface modifiers. This catalytic system avoided the accumulation of hydroxyl amines and their potential exothermic decomposition during the reaction.[4] It is widely reported in the literature that supported gold nanoparticles as well as colloidal gold are very efficient catalysts for the selective reduction of nitro group even in the presence of other reducible groups mostly under mild reaction conditions.[5] In a very recent report Choi *et al.* have shown that hybrid gold nanoparticles on reduced graphene oxide nanosheets selectively reduce nitroarenes.[5a] Gold nanostructures on tannic acid functionalized graphene oxide have been shown to be an effective catalyst for 4-nitrophenol reduction.[5b] Han *et al.* reported that gold nanoparticles supported on polyaniline fibres catalyze the reduction of 4-nitrophenol.[5c] Gold nanoparticles supported on micro structured paper matrix were also shown to be highly efficient for the reduction of 4-nitrophenol.[5d] Gold (as well as silver) nanoparticles stabilized on calcium alginate gel beads reduce 4-nitrophenol using excess $NaBH_4$.[5e] Esumi *et al.* synthesized gold dendrimer nanocomposites by laser irradiation and employed it for catalyzing the reduction of 4-nitrophenol using $NaBH_4$.[5f] Amphiphilic ionic liquid terminated gold nanorods were found to be effective for the reduction of nitro compounds using KBH_4.[5g] Pradhan *et al.* demonstrated the reduction of nitroarenes catalyzed by coinage metal (copper, silver and gold) nanoparticles and $NaBH_4$ in aqueous or micellar medium.[5h] Bayberry tannin-stabilized gold nanoparticles immobilized onto porous alumina is also reported to be an efficient

[a]Inorganic and Physical Chemistry Division, Indian Institute of Chemical Technology, Hyderabad-500607, India. E-mail: mlakshmi@iict.res.in; Fax: +91-40-27160921; Tel: +91-40-27193510
[b]Research Center for Compact Chemical System, National Institute of Advanced Industrial Science and Technology (AIST), 4-2-1 Nigatake, Miyagino, Sendai 983-8551, Japan
[c]Institute of Solid State Physics, The University of Tokyo, 5-1-5 Kashiwanoha, Kashiwa, Chiba, 277-8581, Japan
[d]Department of Complexity Science and Engineering, Graduate School of Frontier Sciences, The University of Tokyo, 5-1-5 Kashiwanoha, Kashiwa, Chiba, 277-8561, Japan
†Electronic supplementary information (ESI) available: General remarks, TEM images of meso HAP–Au(0) and meso CeO₂–Au(0) catalysts, EXAFS studies of meso HAP–Au(0) and meso CeO₂–Au(0) catalysts, spectroscopic characterization (¹H NMR, ¹³C NMR and mass spectral data) of products. See DOI: 10.1039/c2gc35917k
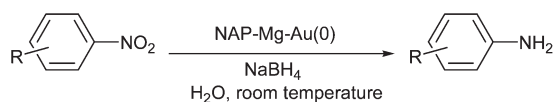
Scheme 1 NAP-Mg–Au(0) catalyzed reduction of nitroarenes in the presence of sodium borohydride in aqueous medium at room temperature.

heterogeneous catalyst for the reduction of 4-nitrophenol to 4-aminophenol.[5i]

In this paper, we report gold nanoparticles supported on commercially available Nano Active™ Magnesium Oxide Plus (NAP-MgO) as a heterogeneous catalyst for the efficient reduction of nitroarenes containing various functional groups in aqueous medium at room temperature with sodium borohydride as the source of hydrogen (see Scheme 1).

Results and discussion

The NAP-MgO support possesses certain physical and chemical properties[6] that enable it as a very suitable support for heterogenizing metal nanoparticles. For example, the presence of various edge corner defect sites with Mg^{2+} (Lewis acidic) or O^{2-} (Lewis basic) sites, along with various cationic and anionic vacancies in the nanocrystalline lattice enables NAP-MgO to possess high concentration of reactive surface ions. These sites are well exposed during the reaction which enables both the substrates and the metal nanoparticles that are stabilized on to these charged sites to promote facile attack of reactants so as to afford the desired product in high yields for a variety of important chemical reactions.[7] XRD studies reveals that the chemically most reactive (111) plane of nanostructured magnesium oxide[8] possesses the maximum concentration of catalytically active gold species thus making it a very efficient catalyst for chemical reactions.

Synthesis of the NAP-Mg–Au(0) catalyst

NAP-Mg–Au(0) catalyst is synthesized according to a procedure reported earlier.[7a] Nano Active™ Magnesium Oxide Plus was purchased from Nano Scale Corp. (Manhattan, USA). It was then calcined at 450 °C for four hours in air. The BET specific surface area for the calcined sample was determined to be 81 m^2 g^{-1}. To incorporate gold species on the surface of NAP-MgO, an ion-exchange reaction was carried out between $HAuCl_4$ and NAP-MgO, and then the exchanged gold species were reduced using excess of sodium borohydride to obtain Au(0) nanoparticles that are deposited on to NAP-MgO support.

Characterization of the NAP-Mg–Au(0) catalyst

The synthesized NAP-Mg–Au(0) catalyst was thoroughly characterized by various sophisticated analytical techniques such as TEM, XRD, XPS, EDX, FT-IR and BET specific surface area studies as reported earlier.[7a] The transmission electron micrograph (TEM) images of the NAP-Mg–Au(0) catalyst show an almost good dispersion of Au(0) nanoparticles on the NAP-MgO support. The average size of the Au(0) nanoparticles
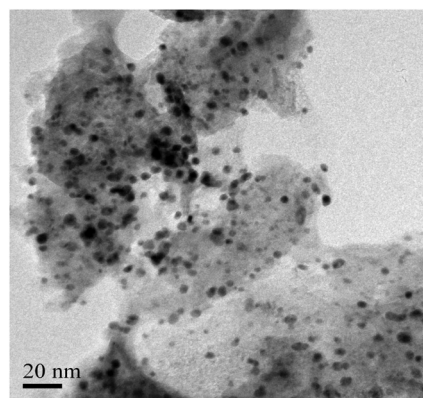

Fig. 1 Bright Field Transmission Electron Micrograph (TEM) image of NAP-Mg–Au(0) catalyst.
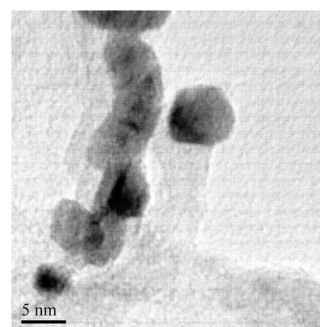
Fig. 2 High Resolution Transmission Electron Micrograph (HRTEM) image of NAP-Mg–Au(0) catalyst.

from TEM studies is determined to be in the range of 5–7 nm (see Fig. 1). The high resolution TEM (HRTEM) image of NAP-Mg–Au(0) catalyst is also given in Fig. 2 wherein the size of a single Au particle matches with that of the average size obtained from TEM image in Fig. 1. TEM images of meso-HAP–Au(0) (HAP: hydroxyapatite) and meso-CeO$_2$–Au(0) have also been recorded and the results can be seen in the ESI.† X-ray diffraction (XRD) studies on the NAP-MgO support revealed the presence of both cubic crystalline phases of magnesium oxide as well as hexagonal crystalline phases of hydrated magnesium oxide. The XRD planes of NAP-Mg–Au(0) match the face centered cubic (fcc) crystalline phase of gold nanoparticles (see Fig. 3). The survey scan X-ray photoelectron spectroscopy (XPS) of the NAP-Mg–Au(0) catalyst is shown in Fig. 4(a). The high resolution narrow scan of this catalyst (see Fig. 4(b)) shows two peaks at 83.9 eV and 87.9 eV, which are characteristic of $4f_{7/2}$ and $4f_{5/2}$ peaks of Au(0) nanoparticles. The energy dispersive X-ray (EDX) studies of the NAP-Mg–Au(0) catalyst have also been performed and it reveals the presence of 1.34% of atomic gold in NAP-Mg–Au(0) catalyst which matches well with that obtained from inductively coupled plasma-optical emission spectrometry (ICP-OES) analysis. The FT-IR studies of the NAP-MgO support as well as the NAP-Mg–Au(0) catalyst have also been carried out (see Fig. 5). The presence of non-bonded OH groups at 3699 cm^{-1} indicates that the surface of nanocrystalline magnesium oxide becomes entirely hydroxylated during its
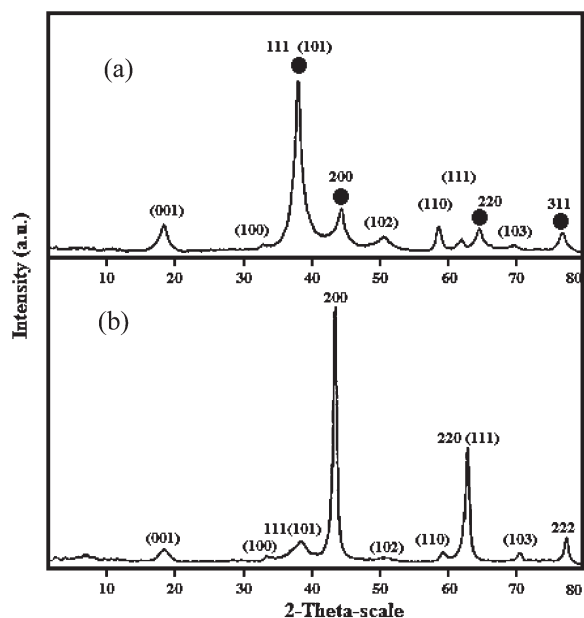
Fig. 3 Powder X-ray diffraction (XRD) pattern of (a) NAP-Mg–Au(0) catalyst (the figures in parentheses show the diffraction from planes corresponding to hydrated hexagonal crystalline phases of NAP-MgO and those without parentheses (also indexed with solid black dots) indicate the planes corresponding to cubic crystalline phases of Au(0) nanoparticles) and (b) NAP-MgO (the figures in parentheses indicate the planes corresponding to hydrated hexagonal crystalline phases of NAP-MgO, and those without parentheses indicate the planes corresponding to cubic crystalline phases of NAP-MgO).

preparation. This is consistent with the reactive profile of NAP-MgO with water.[9] Measurements of Au–L_{III} edge extended X-ray absorption fine structure (EXAFS) were carried out in order to characterize the coordination states of the NAP-Mg–Au(0) catalyst. The measured and fitted k^3-weighted Fourier transforms of the Au–L_{III} edge EXAFS and summary table for EXAFS fitting results are given in Fig. 6 and Table 1 respectively. From these measurements and analysis, it was found that NAP-Mg–Au(0) exhibits Au–Au metallic bonding with slightly reduced coordination numbers as in an Au foil, indicative of Au metallic nanoparticles. EXAFS details of other supported gold catalysts *viz.* meso-HAP–Au(0) and meso-CeO$_2$–Au(0) are presented in the ESI.† The BET specific surface area obtained for NAP-Mg–Au(0) catalyst was determined to be 47 m^2 g^{-1}.

Optimization of amount of sodium borohydride and gold content in NAP-Mg–Au(0) catalyst for the reduction of 4-nitrophenol

To determine the optimum amount of sodium borohydride and NAP-Mg–Au(0) catalyst required for the reduction of nitroarenes, reduction studies were carried out with varying amounts of NaBH$_4$ and NAP-Mg–Au(0) catalyst using 4-nitrophenol as the representative substrate.

It can be seen from Table 2 that upon keeping the amount of sodium borohydride constant, the time for completion of the reduction of 4-nitrophenol decreases on increasing the gold content in the catalyst. Similarly, upon keeping the gold content
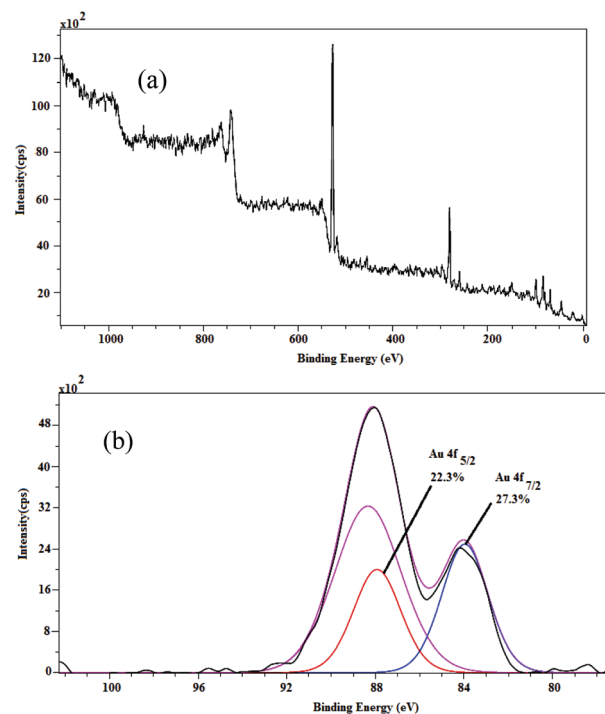
Fig. 4 (a) Survey scan of X-ray Photo Electron Spectra (XPS) of NAP-Mg–Au(0) catalyst. (b) High resolution narrow scan of the same.
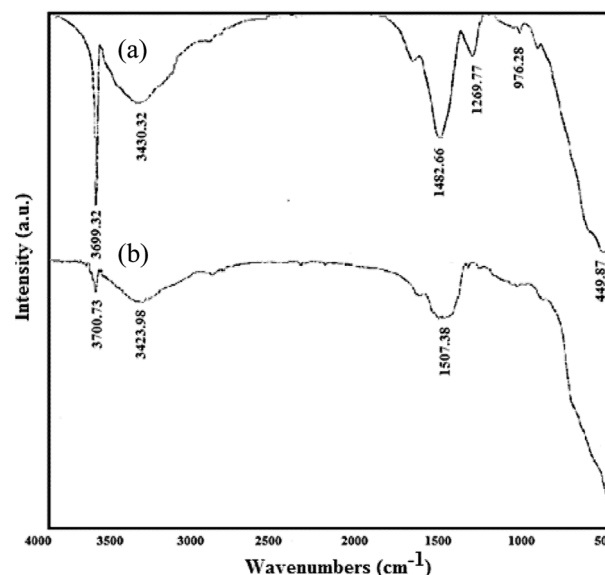
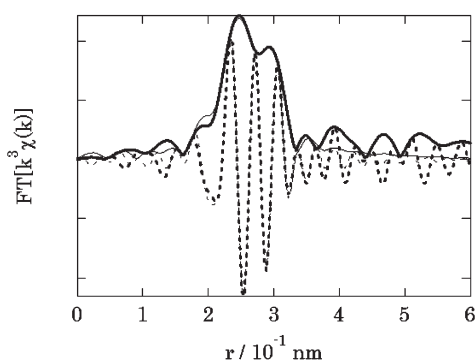**Fig. 5** FT-IR spectra of (a) NAP-Mg–Au(0) catalyst and (b) NAP-MgO.

in the catalyst constant, the time for completion of the reaction decreases on increasing the amount of borohydride reagent. No reaction occurred either in the absence of the gold catalyst or sodium borohydride. To optimize the time duration of the reaction as well as the amount of catalyst and NaBH$_4$ required for the reaction, 15 mg of NAP-Mg–Au(0) catalyst containing 1.34% Au and 0.01 mole of NaBH$_4$ was selected as the optimum amount for reducing 2.156 × 10^{-4} moles of nitroarene.

This experiment is important because an optimum time duration once determined will enable one conveniently to follow the reaction kinetics of the reduction of 4-nitrophenol spectrophotometrically, which will be discussed in the next section.

Evaluation and comparison of the apparent rate constant (k_{app}) of 4-nitrophenol reduction catalyzed by supported gold catalysts

The optimized reaction conditions obtained by employing NAP-Mg–Au(0) catalyst for the reduction of 4-nitrophenol were employed for other supported gold catalysts for kinetic studies. To compare their catalytic activity, the reduction of 4-nitrophenol was tested by UV-Vis spectrophotometric studies and their apparent rate constants were determined. An aqueous solution of 4-nitrophenol gives a peak at 317 nm (λ_{max}),[5e] but on addition of sodium borohydride this peak is red-shifted to 400 nm (λ_{max}) due to the formation of the 4-nitrophenolate ion.[10] On adding the NAP-Mg–Au(0) catalyst to this reaction mixture, the absorbance at 400 nm immediately decreases with the gradual development of a new peak at 300 nm (λ_{max})[10] corresponding to the formation of 4-aminophenol. (See Fig. 7(a)) It is important to note here that the reaction started immediately after the addition of the catalyst and no induction time was noticed which is in contrast to other literature reports involving Pt, Pd and Ag nanocomposites[11] for the reduction of nitro groups. The induction time usually arises from the reaction of dissolved O_2 in water with $NaBH_4$ rather than with 4-nitrophenol.[5e] In our case this was averted by stirring the reaction contents under a N_2 balloon for 15 minutes prior to the addition of the catalyst. The yellow colour of the 4-nitrophenol solution discharged in 7 minutes under continuous stirring signalling the completion of the reaction.

Esumi et al. has proposed that the catalytic reduction of 4-nitrophenol with $NaBH_4$ proceeded in two steps: (1) diffusion and adsorption of 4-nitrophenol to the gold surface and (2) electron transfer mediated by the Au surface from BH_4^- to 4-nitrophenol.[5f] A strong nucleophile such as $NaBH_4$ because of its diffusive nature and high electron injection capability transfers electrons to the substrates via metal particles. This helps to overcome the kinetic barrier of the reaction.[5h] When Au free NAP-MgO was used as the catalyst the reaction did not proceed at all within the optimized time frame (see Fig. 8). This clearly proves that gold nanoparticles deposited on NAP-MgO are an efficient catalyst for 4-nitrophenol reduction. The catalytic activity of meso-HAP–Au(0) and meso-CeO$_2$–Au(0) were also investigated for the reduction of 4-nitrophenol. A definite amount of the catalyst containing an equivalent amount of gold as that present in the NAP-Mg–Au(0) catalyst was used to evaluate their catalytic activity. As can be seen from Fig. 7(c) and (e), meso-HAP–Au(0) and meso-CeO$_2$–Au(0) took almost similar time to complete the reaction. A clear isosbestic point could not be obtained in the spectra. The most likely cause for this might be the evolution of hydrogen bubbles from the reaction mixture which interferes in the spectrophotometric studies and leads to a shift in the UV-visible spectra.[12] Due to the presence of large excess of $NaBH_4$ compared to 4-nitrophenol, the rate of reduction is independent of the concentration of $NaBH_4$, and the reaction could be considered pseudo-first order with respect to the concentration of 4-nitrophenol.[13] As the absorbance of 4-nitrophenol is proportional to its concentration in the medium, the ratio of the absorbance at time 't' (A_t) to that at $t = 0$ (A_0) is proportional to the concentration at time 't' (C_t) to that at $t = 0$ (C_0) i.e. $A_t/A_0 \propto C_t/C_0$. The apparent first-order rate law can be

Fig. 6 k^3-weighted Fourier transform of Au–L$_{III}$ edge EXAFS for NAP-Mg–Au(0) catalyst. Amplitude: solid curves; imaginary part: dotted curves; observed data: thick curves; fitting data: thin curves.

Table 2 Optimization of the amount of NAP-Mg–Au(0) catalyst and sodium borohydride for the reduction of 4-nitrophenol[a]

| Entry	Amount of NAP-Mg–Au(0) catalyst (mg) containing 1.34% Au	Amount of sodium borohydride (mol)	Reaction time (min)
1	5	0.01	18
2	10	0.01	8.5
3	15	0.005	11
4	15	0.01	7
5	15	0.015	5.5
6	15	0.02	2.5
7	20	0.01	4
8	25	0.01	2.5
9	–nil–	0.01	No reaction
1.	15	–nil–	No reaction

[a] Reaction conditions: 2.156×10^{-4} moles of 4-nitrophenol and given amount of $NaBH_4$ was stirred in aqueous medium at room temperature for 15 minutes under a N_2 balloon prior to the addition of the given amount of NAP-Mg–Au(0) catalyst. Time was calculated from the addition of the catalyst until the disappearance of the yellow colour of 4-nitrophenol solution.

Table 1 Summary of the EXAFS fitting results for the NAP-Mg–Au(0) catalyst

	Au–Au, R (10^{-1} nm)	CN	DW (10^{-5} nm^2)	Δk (10 nm^{-1})	Δr (10^{-1} nm)	ΔE_0 (eV)	R_f (%)
Au foil	2.857 ± 0.019	11.4 ± 0.5	8.0 ± 0.2	3.0–16.0	1.0–3.0	0.5 ± 0.5	0.46
NAP-Mg–Au (0)	2.845 ± 0.058	8.4 ± 1.1	8.4 ± 0.9	3.0–11.0	1.0–3.2	3.3 ± 1.0	1.15
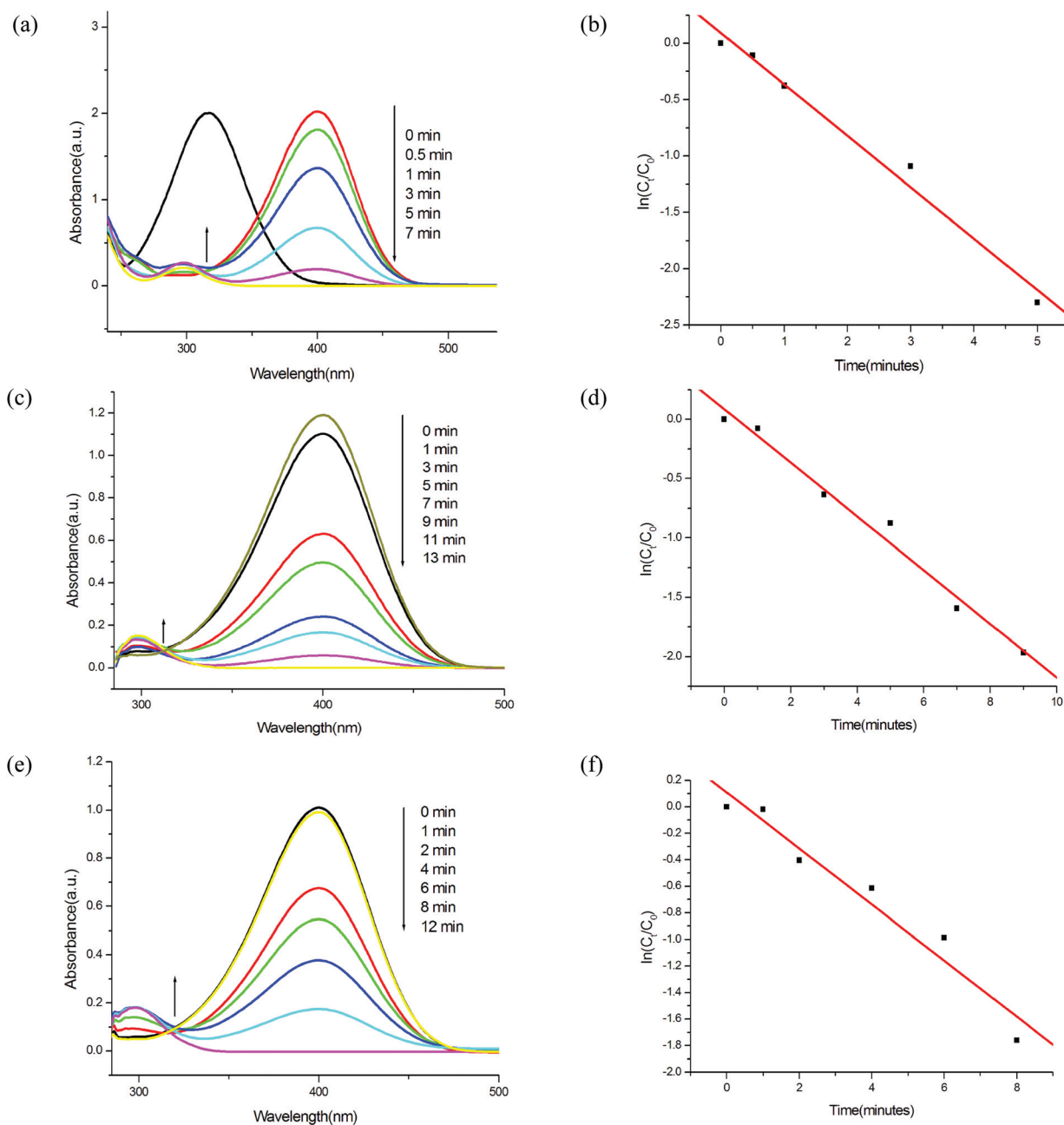
Fig. 7 (a, c & e) Time-dependent UV-visible absorption spectra for the reduction of 4-nitrophenol over (a) NAP-Mg–Au(0), (c) meso-HAP–Au(0), and (e) meso-CeO$_2$–Au(0) catalysts in aqueous media at room temperature. (b, d & f) Plot of ln(C_t/C_0) *versus* time for the reduction of 4-nitrophenol with (b) NAP-Mg–Au(0), (d) meso-HAP–Au(0), and (f) meso-CeO$_2$–Au(0) catalyst.

fitted reasonably well to nearly 90% of the conversion for the reaction. The last data point that is corresponding to 100% conversion did not fall along the linear line (see ESI†). This non-linearity that arises towards the end of the reaction may perhaps be due to the manifestation of multiple orders which come into play due to the presence of various reaction intermediates that might be involved during the course of the reaction. The linear fit of ln C_t/C_0 *vs.* time plots were thus limited to 90% of the obtained data points. From the slope of the line obtained by plotting ln C_t/C_0 *vs.* time, (see Fig. 7(b), (e) and (f)) the apparent rate constant (k_{app}) for the reduction of 4-nitrophenol could be obtained for all

the three catalysts. For the NAP-Mg–Au(0) catalyst, k_{app} was found to be 7.6×10^{-3} s^{-1} whereas meso-HAP–Au(0) and meso-CeO$_2$–Au(0) gave considerably lower k_{app} values. A comparison of the k_{app} values has been provided in Table 3. From these values it can be concluded that the NAP-Mg–Au(0) catalyst is superior than the other two supported catalysts for the reduction of 4-nitrophenol. This may be attributed to the unique physical and chemical properties possessed by NAP-MgO support coupled with the preferential homogeneous deposition of gold nanoparticles on the catalytically more reactive NAP-MgO support.
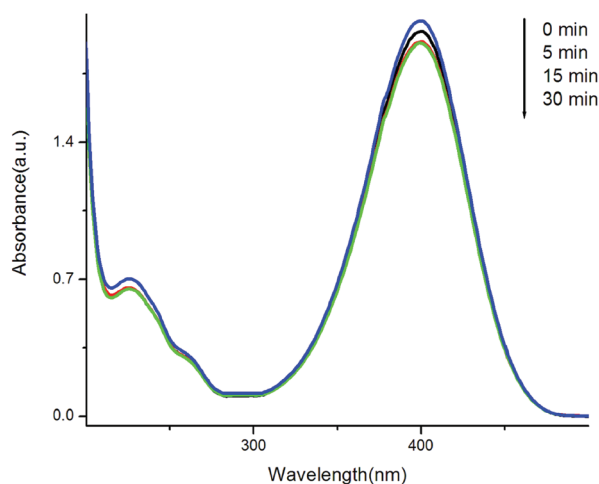
Fig. 8 Time-dependent UV-visible absorption spectra for the reduction of 4-nitrophenol over NAP-MgO.

Table 3 Comparison of k_{app} with different supported gold catalysts for the reduction of 4-nitrophenol

Catalyst	k_{app} ($\times 10^{-3}$ s^{-1})	Error limits
NAP-Mg–Au(0)	7.6	±0.032
Meso-HAP–Au(0)	4.4	±0.085
Meso-CeO$_2$–Au(0)	3.5	±0.023

Catalytic performance of the NAP-Mg–Au(0) catalyst for the reduction of various nitroarenes

To examine the scope of the NAP-Mg–Au (0) catalytic system for the reduction of the nitro group, a series of nitroarenes with structurally divergent functional groups were examined. The catalytic system was found to be very efficient regardless of the presence of electron-withdrawing or electron-donating substituents in the aromatic ring. Simple unsubstituted nitrobenzene yielded the desired aniline product in 60 minutes in 85% yield (Table 4, entry1). 2-, 3- and 4-nitrophenols gave excellent yields of the corresponding anilines in a very short span of time (Table 4, entries 2–4). 3-nitrophenol was found to be the most reactive among all the three nitrophenols. The most obvious reason for this is that since the reaction proceeds through the formation of nitrophenolate ion, 4-nitrophenolate ion is the most stable among all of them because the negative charge on the oxygen atom is effectively delocalised throughout the benzene ring and the system becomes resonance stabilized. 2-Nitrophenol is somewhat less stable than 4-nitrophenol because of less effective resonance coupled with certain degree of steric effect. On the other hand, in 3-nitrophenol, the resonance effect is entirely absent other than through conjugation. So it is the least stable and the most reactive among all the three nitrophenols.[14] This observation is similar to that reported by Choi *et al.* using hybrid gold nanoparticles on reduced graphene oxide nanosheets.[5a] For compounds with two nitro groups, *i.e.* 1, 2-dinitrobenzene and 1, 4-dinitrobenzene (Table 4, entries 5 & 7), one nitro group was selectively reduced though di-amino products were also formed in minor quantities. 3-Nitroaniline was also quite easily reduced

to its corresponding aniline in only 20 minutes (Table 4, entry 6). Halogen substituted nitroarenes were selectively reduced to their corresponding halo anilines in good to excellent yields and no dehalogenation of the product was observed (Table 4, entries 8–15). It was seen that *ortho*-substituted halo nitroarenes displayed somewhat poor reactivity compared to their para-substituted counterparts (Table 4, entries 8, 9 & 12). This proves that our catalytic system is sensitive to steric effects which are similar to that observed by Lou *et al.* using ammonium formate and Au/TiO$_2$ as a catalyst.[5k] Interestingly nitro aromatics with more than one substituted halogen also yielded modest amounts of the respective anilines albeit at longer reaction times (Table 4, entries 14 & 15). The NAP-Mg–Au(0) catalytic system chemoselectively reduced 4-nitrobenzonitrile to 4-aminobenzonitrile without affecting the –CN group (Table 4, entry 16). Nitroarenes possessing electron-donating groups such as *p*-toluidine and *p*-anisidine also afforded excellent yields of the corresponding product (Table 4, entries 17 and 18). Methyl 4-nitrobenzoate was also selectively reduced to its corresponding aniline in good yields and the carbonyl group remained unaffected (Table 4, entry 19) during the reaction. Similarly 3-nitrostyrene could also be reduced to 3-vinylaniline in good yields although 3-ethylaniline was also formed as a side product (Table 4, entry 20).

Probable reaction mechanism for the reduction of nitroarenes catalyzed by the NAP-Mg–Au(0) catalyst and sodium borohydride

Zhang *et al.* studied the reduction of 4-nitrophenol with sodium borohydride catalyzed by silver nanoclusters supported on TiO$_2$[15] and provided a mechanistic investigation which implied that it was modelled in terms of the Langmuir–Hinshelwood mechanism.[16] Similar kinetic investigations were performed by Wunder *et al.* where he studied the kinetic analysis of the catalytic reduction of 4-nitrophenol by Au/Pt nanoparticles immobilized in spherical polyelectrolyte brushes.[12] This mechanism can also be extended to the reduction of aromatic nitroarenes in general and although the exact mechanism of this reduction has not yet been fully explored, we propose a probable surface reduction mechanism based on the Langmuir–Hinshelwood model without going into the intricate kinetic details and stoichiometric equations, using NAP-Mg–Au(0) and sodium borohydride as the catalytic system (see Scheme 2).

First, sodium borohydride ionises in aqueous medium with the generation of borohydride ions which adsorb onto the surface of the gold nanoparticle and react to form a gold hydride complex. Nitrobenzene also adsorbs onto the gold nanoparticle surface and both of these processes are reversible *i.e.*, adsorption accompanied by desorption. Once both the substrates are chemisorbed onto the gold nanoparticle surface there is a hydrogen transfer from the gold hydride complex to the nitrobenzene. Now there are two probable routes for the reduction of nitro group to amino group based on the electrochemical model as presented by Haber – the direct route and the condensation route (see Scheme 3).[17] In the direct route, the aromatic nitro compound is reduced to the nitroso compound and then further to the corresponding hydroxylamine in two very fast consecutive steps. Finally, the hydroxylamine is reduced to the aniline

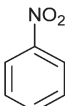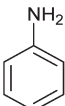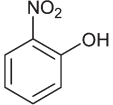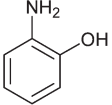**Table 4** Reduction of various nitroarenes catalyzed by NAP-Mg–Au(0)[a]
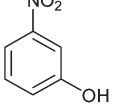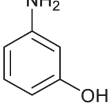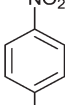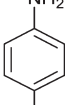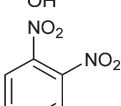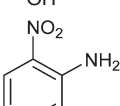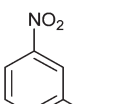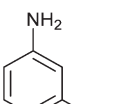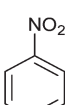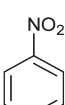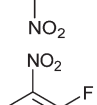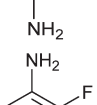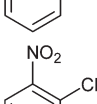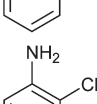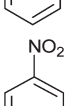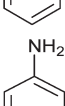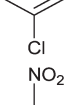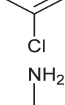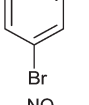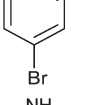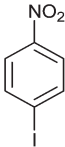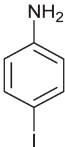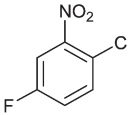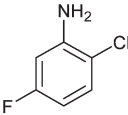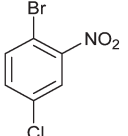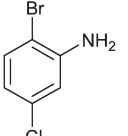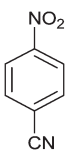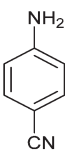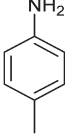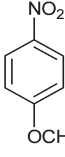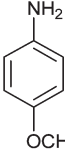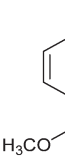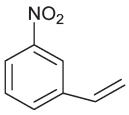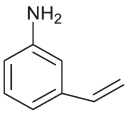
Entry	Substrate	Product	Time (min)	Conversion/selectivity[b] (%)	Yield[c] (%)
1	NO$_2$ (benzene)	NH$_2$ (benzene)	60	98/91	85
2	NO$_2$, OH	NH$_2$, OH	3	100/100	99[d]
3	NO$_2$, OH	NH$_2$, OH	1	100/100	99[d]
4	NO$_2$, OH	NH$_2$, OH	7	100/100	98 (TON = 207.05)[d,g]
[e]5	NO$_2$, NO$_2$	NO$_2$, NH$_2$	45	100/82	78
6	NO$_2$, NH$_2$	NH$_2$, NH$_2$	20	100/100	98[d]
[f]7	NO$_2$, NO$_2$	NO$_2$, NH$_2$	70	100/77	74
8	NO$_2$, F	NH$_2$, F	150	97/85	77
9	NO$_2$, Cl	NH$_2$, Cl	240	84/87	68
10	NO$_2$, Cl	NH$_2$, Cl	80	95/91	81
11	NO$_2$, Br	NH$_2$, Br	60	97/93	85
12	NO$_2$, I	NH$_2$, I	240	70/84	55

Table 4   *(Contd.)*

Entry	Substrate	Product	Time (min)	Conversion/selectivity[b] (%)	Yield[c] (%)
13			80	98/97	92
14			240	90/87	74
15			240	91/91	78
16			90	94/98	87
17			60	100/94	88
18			80	100/95	91
19			90	96/89	80
20			120	100/85	81

[a] Reaction Conditions: 1.078×10^{-3} moles of nitroarene and 0.05 mole of $NaBH_4$ were stirred in 10 mL of double distilled water at room temperature under a N_2 balloon for 15 minutes. Then 75 mg of NAP-Mg–Au(0) catalyst was added and the contents were allowed to stir for the appropriate amount of time. [b] Analysed by GC. [c] Isolated yields after column chromatography. [d] Yield after work up. [e] 15% of diamine minor product. [f] 21% of diamine minor product. [g] Turnover Number (TON) calculated as moles of product formed/moles of catalyst used.
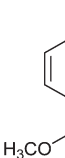
derivative in the rate determining step (direct route, see top in Scheme 3). The second route proposed involves the condensation of one molecule of the nitroso compound with a molecule of the hydroxylamine to give the azoxy compound, which in turn gets reduced in a series of consecutive steps to the azo, hydrazo, and aniline compounds (condensation route, see top of Scheme 3). Corma *et al.* have beautifully demonstrated that the direct route is the preferred pathway for the hydrogenation of aromatic nitro compounds on the Au/TiO2 catalyst system.[18] To obtain an insight into the reaction pathway involved in NAP-Mg–Au(0) catalyzed reduction, the reaction intermediates involved in both the routes were separately subjected to a

reduction process using the NAP-Mg–Au(0) catalyst. When nitrosobenzene was subjected to reduction it yielded about 70% of aniline in 45 minutes. TLC studies did not show any traces of unreacted nitrosobenzene but phenyl hydroxylamine was present in the reaction mixture which decreased with time to yield more of the desired product. The absence of nitrosobenzene in the reaction mixture signifies that it gets very strongly adsorbed onto the catalyst surface and reacts before desorption. Also it demonstrates that the reduction of nitrosobenzene is faster compared to that of the reduction of phenylhydroxylamine and thus this reaction step might be the rate determining step. The absence of azobenzene in the reaction mixture probably signifies that the
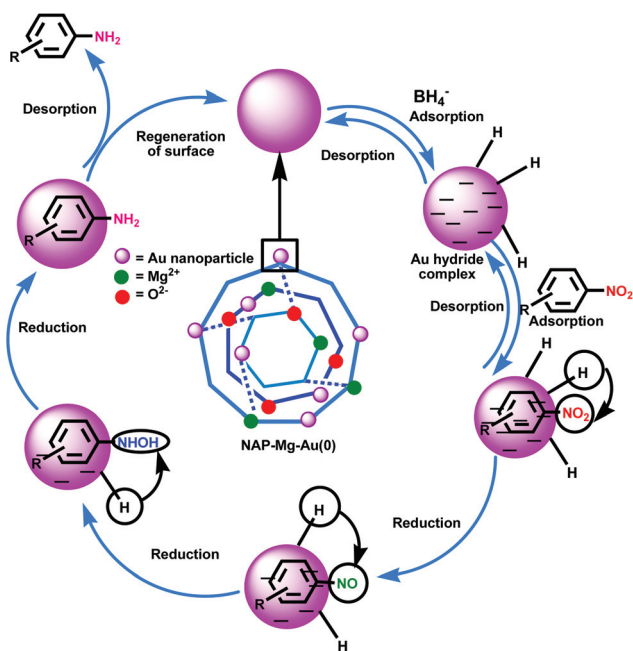
Scheme 2 Probable reaction mechanism for the reduction of nitroarene catalyzed by the NAP-Mg–Au(0) catalyst and sodium borohydride.
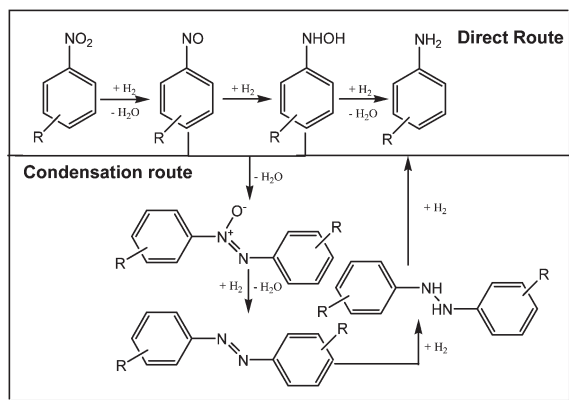
Scheme 3 Proposed reaction pathways for the reduction of aromatic nitro group to amino group.

condensation route is not the preferred one for reduction. To further verify this observation azobenzene was also separately subjected to reduction and as expected there was no product formation even after 45 minutes. Thus it may be concluded that the direct route involving nitrobenzene → nitrosobenzene → phenyl-hydroxylamine → aniline is the most likely path followed for the reduction of aromatic nitro group involving NAP-Mg–Au(0) catalyst. These reactions occur on the surface of gold nanoparticle and once aniline is formed it desorbs from the surface to create a free surface and the catalytic cycle starts again.

Reusability studies of the NAP-Mg–Au(0) catalyst and kinetic analysis on the conversion of nitrobenzene

The reusability studies of the NAP-Mg–Au(0) catalyst was carried out with nitrobenzene as the model substrate. $2.156 \times$

**Table 5** Reusability studies of the NAP-Mg–Au(0) catalyst[a]

Reaction cycle	1st	2nd	3rd	4th	5th
Weight of catalyst (mg)	150	147	143	139	133
Conversion of nitrobenzene (%)[b]	98	96	93	90	86
Yield (%)[c]	86	84	82	79	75
k_{app} (min^{-1})	0.063	0.053	0.044	0.038	0.034
Error limits ($\times 10^{-3}$)	±4.85	±3.22	±2.33	±1.78	±1.30

[a] 2.156×10^{-3} moles of nitrobenzene and 0.1 mole of NaBH$_4$ were allowed to stir in 15 mL of double distilled water at room temperature under a N$_2$ balloon for 15 minutes. To this a given amount of the NAP-Mg–Au(0) catalyst was added and the contents were allowed to stir for another 1 hour. [b] Analysed by GC. [c] Isolated yield of aniline after column chromatography.
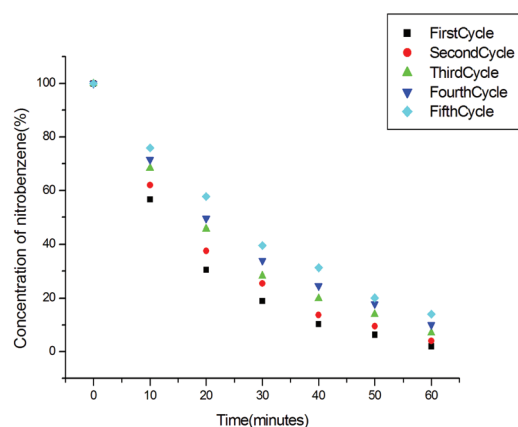

Fig. 9 Conversion of nitrobenzene with time using the NAP-Mg–Au(0) catalyst.

10^{-3} moles of nitrobenzene and 0.1 mole of NaBH$_4$ were allowed to stir in 15 mL of double distilled water at room temperature under a N$_2$ balloon for 15 minutes. To this 150 mg of NAP-Mg–Au(0) catalyst was added and the contents were allowed to stir for another 1 hour. After the completion of the reaction, the contents were centrifuged to separate the solid catalyst from the reaction mixture. The catalyst was then thoroughly washed with distilled water followed by acetone and then dried in air. After drying, the catalyst was weighed. A slight drop in weight of the catalyst was recorded after each cycle (see Table 5). This catalyst was used for another four reaction cycles. The conversion of nitrobenzene was monitored with time for every cycle to determine the activity of the NAP-Mg–Au(0) catalyst (see Fig. 9). As the reaction can be considered to follow pseudo first order kinetics with respect to the concentration of nitrobenzene, the apparent rate constant (k_{app}) for each reaction cycle can be calculated from the slope by obtaining a linear fit of ln (C_t/C_0) (C_t: concentration of nitrobenzene at time = 't'; C_0 = concentration of nitrobenzene at time 't' = 0) vs. time (see Fig. 10). From Table 5, it can be seen that there is a gradual decrease in k_{app} with every reaction cycle. Primarily it may be assigned to the gradual loss in weight of the catalyst during recycling or may be attributed to changes in particle size or crystalline structure of the catalyst on repeated use. To confirm this, the
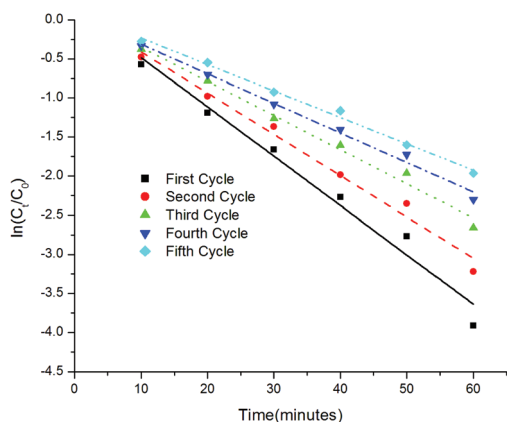
Fig. 10 Plots of $\ln(C_t/C_0)$ *vs.* time for the conversion of nitrobenzene with th eNAP-Mg–Au(0) catalyst.
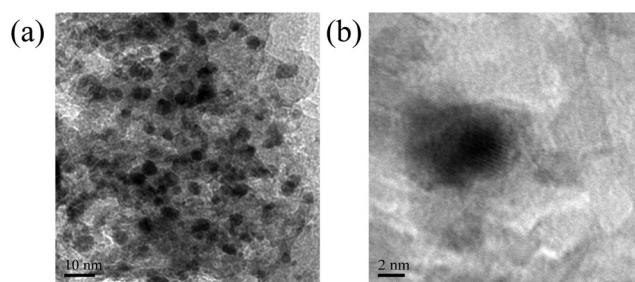

Fig. 11 (a) TEM image of used NAP-Mg–Au(0) catalyst (after five reaction cycles) and (b) HRTEM image of the same.

used catalyst (after five cycles) was subjected to TEM, HRTEM and XRD analyses (see Fig. 11 and 12).

The TEM image of used NAP-Mg-Au(0) catalyst (see Fig. 11 (a)) shows the dispersion of the Au nanoparticles on the support and does not indicate any appreciable agglomeration of the particles even after five reaction cycles. This fact is further supported by the HRTEM image (see Fig. 11(b)) of a single Au particle of the used catalyst. The XRD peaks of the used catalyst (see Fig. 12) does not show any change thereby demonstrating that the morphology of the catalyst remains intact even after five reaction cycles. So the decrease in k_{app} for the conversion of nitrobenzene with every reaction cycle may be largely attributed to the loss in catalyst during recycling. This observation is similar to that reported by Han *et al.* where they showed a gradual decrease in k_{app} values with every reaction cycle for the reduction of 4-nitrophenol catalyzed by Au nanoparticles supported on polyaniline fibres and $NaBH_4$ and attributed this decrease to the loss of catalyst arising from separation and purification processes.[5c]

Heterogeneity studies of the NAP-Mg–Au(0) catalyst

To verify whether the reduction of nitroarene catalyzed by the NAP-Mg–Au(0) catalyst follows a heterogeneous pathway, 2.156×10^{-4} moles of nitrobenzene were subjected to reduction using 0.01 mole of $NaBH_4$ and 15 mg of catalyst in 5 mL of double distilled water at room temperature. After 10 minutes of
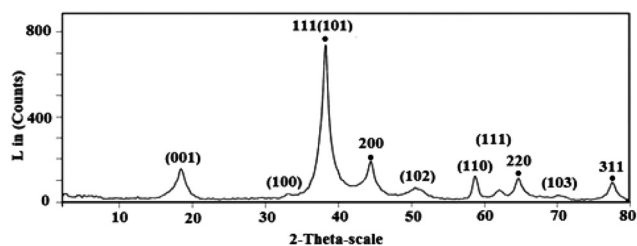
Fig. 12 Powder X-ray diffraction (XRD) pattern of the used NAP-Mg–Au(0) catalyst after five reaction cycles (the figures in parentheses show the diffraction from planes corresponding to hydrated hexagonal crystalline phases of NAP-MgO and those without parentheses (also indexed with solid black dots) indicate the planes corresponding to cubic crystalline phases of Au(0) nanoparticles).

reaction, when the concentration of nitrobenzene was about 57%, the catalyst was separated from the reaction mixture and the reaction continued. There was no change in the conversion of nitrobenzene even after 30 minutes. The filtrate was analyzed by ICP-OES for any traces of gold but it was found well below the detection limit. The gold content in the used catalyst also matched well with that of the fresh catalyst. This proves that during the course of the reaction there was no leaching of gold from the solid support and the reaction followed a heterogeneous pathway.

Conclusion

In conclusion, Au(0) nanoparticles of 5–7 nm size that are heterogenized onto a commercial NAP-MgO support, [(NAP-Mg–Au(0)], performs efficiently as a recyclable heterogeneous catalytic system for the chemoselective reduction of aromatic nitroarenes in aqueous medium at ambient temperature. This catalytic system effectively reduces the nitro group to an amino group in good to excellent yields without affecting other vulnerable groups such as halo, carbonyl or nitrile groups present in the benzene ring. Also, no additives or promoters are needed for the reaction. The UV-visible spectrophotometric studies on 4-nitrophenol were also performed and an apparent rate constant of 7.6×10^{-3} s^{-1} was obtained for the NAP-Mg–Au(0) catalyst which is found to be considerably higher when compared to the other supported gold catalysts used in our studies. These key findings make the nanotechnology based recyclable heterogeneous catalysis platform provided herein inherently advanced, economical, green and environmentally sustainable for the reduction of aromatic nitroarenes.

Experimental

Synthesis of the NAP-Mg–Au(0) catalyst

Commercial NAP-MgO was calcined at 450 °C for four hours in air. This NAP-MgO support (3.5 g) was treated with chloroauric acid solution (1 g, 2.54 mmol; dissolved in 100 mL of double distilled water), and stirred at 25 °C for 12 h under nitrogen atmosphere to give Au(III)-exchanged NAP-Mg–Au(III) species. To this reaction mixture, excess of sodium borohydride (3.5 g, 92.5 mmol) was slowly added and the contents were allowed to

stir under nitrogen atmosphere for another 12 h. The solid catalyst was then filtered through G-3 sintered glass funnel, washed thoroughly with double distilled water and then with acetone. It was then oven dried at 70 °C to obtain NAP-Mg–Au(0) as a dark purple coloured powder. Similar synthetic procedures were adopted for meso-HAP–Au(0) and meso-CeO$_2$–Au(0) catalysts.[19]

General procedure for the spectrophotometric determination of the reduction of 4-nitrophenol over NAP-Mg–Au(0) and other supported gold catalysts

2.156×10^{-4} moles of 4-nitrophenol were dissolved in 5 mL of double distilled water to give a yellow coloured solution. To it 0.01 mole of sodium borohydride was added and allowed to stir under a nitrogen balloon for 15 minutes. Then 15 mg of NAP-Mg–Au(0) catalyst (or equivalent weight of other supported catalysts containing the same amount of gold) was added and stirring continued. Just after the addition of the catalyst, a small portion of the reaction mixture was withdrawn and its absorbance recorded by a UV-visible spectrophotometer. The process was repeated at regular time intervals until complete discoloration of the solution.

General experimental procedure for the reduction of nitroarenes catalyzed by NAP-Mg–Au(0)

1.078×10^{-3} moles of nitroarene and 0.05 mole of sodium borohydride were stirred in about 10 mL of double distilled water under a nitrogen balloon for 15 minutes. Then 75 mg of NAP-Mg–Au (0) catalyst was added and stirred for the appropriate amount of time. The progress of the reaction was monitored by TLC. After the completion of the reaction, the reaction mixture was centrifuged to separate the catalyst. The solid residue was first washed with distilled water and then with acetone to remove any traces of organic material. It was then dried in air at room temperature and used as it is for further reactions. The filtrate containing the reaction mixture was extracted with ethyl acetate (3 × 10 mL), and then washed with brine solution (10 mL), and dried over anhydrous Na$_2$SO$_4$. The solvent was evaporated under reduced pressure to yield the crude product, which was then purified by column chromatography using silica gel using hexane/ethyl acetate as an eluent to afford the pure product. The products were characterized by both ^{1}H-NMR and ^{13}C-NMR as well as mass spectral studies (see ESI†).

Acknowledgements

References

1. (a) B. Hammer and J. K. Norskov, *Nature*, 1995, **376**, 238; (b) G. C. Bond, *Catalysis by Metals*, Academic Press, London, New York, 1962.
2. P. Claus, *Appl. Catal., A*, 2005, **291**, 222 and the references cited therein.
3. (a) R. S. Dowing, P. J. Kunkeler and H. van Bekkum, *Catal. Today*, 1997, **37**, 121; (b) M. Suchy, P. Winternitz and M. Zeller, *World (WO) Patent 91/00278*, 1991.
4. A. Corma and P. Serna, *Science*, 2006, **313**, 332.
5. (a) Y. Choi, H. S. Bae, E. Seo, S. Jang, K. H. Park and B.-S. Kim, *J. Mater. Chem.*, 2011, **21**, 15431; (b) Y. Zhang, S. Liu, W. Lu, L. Wang, J. Tian and X. Sun, *Catal. Sci. Technol.*, 2011, **1**, 1142; (c) J. Han, L. Li and R. Guo, *Macromolecules*, 2010, **43**, 10636; (d) H. Koga and T. Kitaoka, *Chem. Eng. J.*, 2011, **168**, 420; (e) S. Saha, A. Pal, S. Kundu, S. Basu and T. Pal, *Langmuir*, 2010, **26**, 2885; (f) K. Hayakawa, T. Yoshimura and K. Esumi, *Langmuir*, 2003, **19**, 5517; (g) X. Bai, Y. Gao, H.-g. Liu and L. Zheng, *J. Phys. Chem. C*, 2009, **113**, 17730; (h) N. Pradhan, A. Pal and T. Pal, *Langmuir*, 2001, **17**, 1800; (i) X. Huang, X. Liao and B. Shi, *Green Chem.*, 2011, **13**, 2801; (j) L. He, L.-C. Wang, H. Sun, J. Ni, Y. Cao, H.-Y. He and K.-N. Fan, *Angew. Chem., Int. Ed.*, 2009, **48**, 9538; (k) X.-B. Lou, L. He, Y. Qian, Y.-M. Liu, Y. Cao and K.-N. Fan, *Adv. Synth. Catal.*, 2011, **353**, 281; (l) Y. Chen, J. Qiu, X. Wang and J. Xiu, *J. Catal.*, 2006, **242**, 227.
6. (a) P. Jeevanandam and K. J. Klabunde, *Langmuir*, 2002, **18**, 5309; (b) K. J. Klabunde and R. Mulukutla, *Nanoscale Materials in Chemistry*, Wiley Interscience, New York, 2001, Chapter 7, p. 223.
7. (a) K. Layek, R. Chakravarti, M. L. Kantam, H. Maheswaran and A. Vinu, *Green Chem.*, 2011, **13**, 2878; (b) B. M. Choudary, K. Jyothi, M. Roy, M. L. Kantam and B. Sreedhar, *Adv. Synth. Catal.*, 2004, **346**, 1471; (c) M. L. Kantam, U. Pal, B. Sreedhar, S. Bhargava, Y. Iwasawa, M. Tada and B. M. Choudary, *Adv. Synth. Catal.*, 2008, **350**, 1225; (d) M. L. Kantam, J. Yadav, S. Laha, B. Sreedhar and S. Bhargava, *Adv. Synth. Catal.*, 2008, **350**, 2575; (e) M. L. Kantam, S. Roy, M. Roy, M. S. Subhas, P. R. Likhar, B. Sreedhar and B. M. Choudary, *Synlett*, 2006, 2747; (f) K. Layek, H. Maheswaran, R. Arundhathi, M. L. Kantam and S. K. Bhargava, *Adv. Synth. Catal.*, 2011, **353**, 606; (g) M. L. Kantam, R. Chakravarti, V. R. Chintareddy, B. Sreedhar and S. Bhargava, *Adv. Synth. Catal.*, 2008, **350**, 2544.
8. K. Zhu, J. Hu, C. Kubel and R. Richards, *Angew. Chem., Int. Ed.*, 2006, **45**, 7277.
9. R. M. Narske, K. J. Klabunde and S. Fultz, *Langmuir*, 2002, **18**, 4819.
10. (a) K. Kuroda, T. Ishida and M. Haruta, *J. Mol. Catal. A: Chem.*, 2009, **298**, 7; (b) D. M. Dotzauer, J. Dai, L. Sun and M. L. Bruening, *Nano Lett.*, 2006, **6**, 2268.
11. (a) Y. Mei, G. Sharma, Y. Lu, M. Ballauff, M. Drechsler, T. Irrgang and R. Kempe, *Langmuir*, 2005, **21**, 12229; (b) Y. Mei, Y. Lu, F. Polzer, M. Drechsler and M. Ballauff, *Chem. Mater.*, 2007, **19**, 1062; (c) Y. Lu, Y. Mei, M. Drechsler and M. Ballauff, *Angew. Chem., Int. Ed.*, 2006, **45**, 813; (d) N. Pradhan, A. Pal and T. Pal, *Colloids Surf., A*, 2002, **196**, 247.
12. S. Wunder, F. Polzer, Y. Lu, Y. Mei and M. Ballauff, *J. Phys. Chem. C*, 2010, **114**, 8814.
13. J. Huang, S. Vongehr, S. Tang, H. Lu and X. Meng, *J. Phys. Chem. C*, 2010, **114**, 15005.
14. S. Jana, S. K. Ghosh, S. Nath, S. Pande, S. Praharaj, S. Panigrahi, S. Basu, T. Endo and T. Pal, *Appl. Catal., A*, 2006, **313**, 41.
15. H. Zhang, X. Li and G. Chen, *J. Mater. Chem.*, 2009, **19**, 8223.
16. M. A. Vannice, *Kinetics of Catalytic Reactions*, Springer Science + Business Media Inc., Philadelphia, PA, 2005.
17. F. Haber, *Z. Elektrochem.*, 1898, **22**, 506.
18. A. Corma, P. Concepcion and P. Serna, *Angew. Chem.*, 2007, **119**, 7404.
19. Procedure for preparation of meso ceria and meso HAP have been adapted from P. Ji, J. Zhang, F. Chen and M. Anpo, *J. Phys. Chem. C*, 2008, **112**, 17809.